

Corrosion Inhibition of Mild Steel in Strong Acid Environment by 4-((5,5-dimethyl-3-oxocyclohex-1-en-1-yl)amino)benzenesulfonamide

A.A. Al-Amiery^{a,*}, L.M. Shaker^a, A.A.H. Kadhum^b, M.S. Takriff^b

^aEnergy and Renewable Energies Technology Center, University of Technology, Baghdad 10001, Iraq,

^bDepartment of Chemical and Process Engineering, University Kebangsaan Malaysia, Bangi, 43000, Malaysia.

Keywords:

Sulfanilamide
Corrosion inhibitor
Mild steel
DFT
DOBF
LUMO

* Corresponding author:

Ahmed Al-Amiery 
E-mail: dr.ahmed1975@gmail.com

Received: 06 August 2019

Revised: 03 October 2019

Accepted: 12 December 2019

ABSTRACT

New sulfanilamide derivative namely 4-((5,5-dimethyl-3-oxocyclohexenyl)amino)benzenesulfonamide (DOBF) was synthesized and the chemical structure was elucidated using Nuclear Magnetic Resonance (NMR) and elemental analysis (CHN). The inhibition effects of a studied DOBF on the corrosion of mild steel in 1 M hydrochloric acid environment were investigated using electrochemical impedance spectroscopy (EIS), weight loss method and scanning electron microscopy (SEM). The synthesized inhibitor concentrations were 0.1 mM to 0.5 mM and the temperatures ranging from 303-333 K. Results showed that the inhibition occurs through adsorption of the inhibitor molecules on the metal surface. Electrochemical and weight loss techniques revealed that the tested DOBF act as superior inhibitor for acidic corrosion of mild steel and the efficiency increase with increasing concentrations. EIS results revealed that DOBF demonstrate the highest inhibition efficiency of 93.70 %, at a concentration of 0.5 mM. The adsorption of the investigated inhibitor obeys Langmuir's adsorption isotherm. Different thermodynamic parameters have been calculated and discussed. SEM confirmed the formation of a protective film on the surface. The investigated techniques are in good agreement to establish the using DOBF as corrosion inhibitor for mild steel in strong acid environment. It was found that the corrosion inhibition performance depends on the concentration of the DOBF and the solution temperature. Quantum chemical calculations have been done to correlate the electronic characteristics of the compounds with the corrosive inhibitive impact. The quantum calculations such as the HOMO, LUMO, energy gap (ΔE), atomic charges, dipole moment (μ), electron affinity (A), chemical hardness (η), softness (σ) electronegativity (χ), ionization potential (I), and fraction of electrons transferred (ΔN), were used to explain the mechanism of inhibition of DOBF molecules on the mild steel surface. Experimental and theoretical results are in good agreement.

1. INTRODUCTION

The most serious problem in the industries that used mild steel was corrosion. In industrial processes that used acidic solutions, every year corrosion problems cost billions, when metal is exposed to corrosive environment. Corrosive environment plays a significant role in industrial process such as; pickling, crude oil refining, scaling, cleaning, and petrochemicals [1]. Different industrial process used highly corrosive environment especially hydrochloric acid. The corrosive conditions could impact the surface of alloys harmfully and decrease the duty life of the equipment's, and hence monitoring and controlling corrosion are permanently required [2,3]. The most actual method to impedance corrosion dissolution of mild steel was the use of corrosion inhibitors. Corrosion inhibitors advantages are lying on the data that they demonstrate superior performance and comparatively low cost due to their economically applicable and simple feasibility behavior [4,5]. Organic molecules containing benzene rings, pi-bonds in addition to hetero-atoms such as nitrogen, phosphorous, sulfur and oxygen are considered to be efficient inhibitors for mild steel corrosion impedance. These organic inhibitors have the abilities to block the corrosion through adsorption on mild steel surface by their electron donating groups. The molecules with corrosive inhibitive characteristics have the ability to react with mild steel surfaces via physi- and/or chemi-sorption mechanism depending on the nature chemical structure of inhibitor molecules and also the nature of mild steel surface [6,7]. Nitrogen, oxygen and sulfur having molecules demonstrated superior protection performance that are resulted because of their lower electronegativities and the ability to form coordination compounds via coordination bonds between high chelating inhibitors and the iron atoms of mild steel surface [8]. Benzenesulfonamides have displayed promising corrosion inhibition for mild steel characteristics in 1M HCl. On comparing the inhibitive efficiencies percentage of benzenesulfonamide with previously reported inhibition efficiencies of various organic compounds in different corrosive environment, it was found that these benzenesulfonamide of this investigation could serve as effective on corrosion inhibition [9]. In the present study,

our significant aim was 3-fold: (i) to examine the influence of benzenesulfonamide containing aromatic ring, heteroatoms (Sulfur, Oxygen and Nitrogen), and α , β -unsaturated carbonyl group on the inhibition behaviors, (ii) to determine the adsorption sites, and (iii) to investigate the influence of concentration, time and temperature on the enhanced inhibitive performances of benzenesulfonamide. To address these issues, and Following up of the investigations for efficient corrosion inhibitors for mild steel in acidic solution [10-32], we designed and synthesized a novel inhibitor from benzenesulfonamide namely 4-((5,5-dimethyl-3-oxocyclohexenyl) amino)benzenesulfonamide (DOBF) on mild steel corrosion in HCl environment, as shown in Fig. 1.

2. EXPERIMENTAL SECTION

2.1 Chemistry

Sigma/Aldrich in Selangor, Malaysia was the supplier for all the solvents and starting materials that were utilized in this study. Spectroscopical analysis for the synthesized compound were done by Nuclear magnetic resonance (NMR) devise and were done through an AVANCE III 600 MHz spectrometer (Bruker, Billerica, Massachusetts, United States of America), with the internal standard namely dimethyl sulfoxide and the sigma values were explained in ppm.

2.2 Synthesis of DOBF as corrosion inhibitor

A mixture of 5,5-dimethyl-cyclohexane-1,3-dione (7.0 g, 5.0 mmol) and sulfanilamide (4.3 g, 2.5 mmol) in 100 mL of ethyl alcohol was stirring and heated at reflux for four hours., The product was cooled and then poured onto ice, isolated and recrystallized from ethyl alcohol. Yield 76%; melting point 237 °C; $^1\text{H-NMR}$ (CDCl_3 , ppm): 1.00 (6H, s, CH_3), 2.08 (2H, d, NH_2), 2.22 (2H, d, CH_2), 2.42 (2H, d, CH_2), 5.64 (1H, s, C=C-H), 6.91 d, 7.35d, 7.49dd and 7.89 d for aromatic ring. CHN analysis for $\text{C}_{14}\text{H}_{18}\text{N}_2\text{O}_3\text{S}$, Cal./Found: C, 57.12/56.93, H, 6.16/5.94 and N, 9.52/9.64.

2.3 Gravimetric Experiments

Metal Samples Company (USA, Pa, Saint) were the supplied of mild steel (MS) specimens that used

for this study. The composition (wt%) mild steel specimens were: 99.210Fe; 0.210C; 0.380 Si; 0.090P; 0.05S; 0.050Mn and 0.010Al. ASTM standard steps G1-03 were used to washed and cleaned the mild steel specimens [33]. Non-stirred 1.0 M hydrochloric acid solution with the different concentration of DOBF.

2.4 Weight Loss Technique

The weight loss measurements have been repeating three times and were proceeding in aerated at the range 303-333 K in 1.0 M HCl (non-stirred) with the concentrations of DOBF 0 mM, 0.1 mM, 0.2 mM, 0.3 mM, 0.4 mM and 0.5 mM. The utilized MS specimens which have rectangular shapes of the dimensions 2.5×2×0.025 cm were suspended hydrochloric acid solution 0.2 L, in presence of the concentrations (0.0, 0.1, 0.2, 0.3, 0.4 and 0.5 mM) of the DOBF. After immersion for 1, 5, 10, 24, 48 and 72 h, the specimens were take-out, washed and dried. The cleaned MS specimens, are weighed accurately. The inhibition efficiency and corrosion rate CR were calculated using eq. 1 and 2 [34, 35]:

$$IE\% = \left[1 - \frac{w_2}{w_1} \right] \times 100 \quad (1)$$

where IE% is *Inhibition efficiency*, W1 is the weight without DOBF and W2 with DOBF:

$$C_R \text{ mm/y} = 87.6W/at\rho \quad (2)$$

where w is the weight loss, a is the area of coupon, and t is the immersion time.

2.5 Electrochemical Impedance Spectroscopy Measurements

EIS measurements have been repeating three times and were proceeding in aerated at the range 303-333 K in 1.0 M HCl (non-stirred) with the concentrations of DOBF 0 mM, 0.1 mM, 0.2 mM, 0.3 mM, 0.4 mM and 0.5 mM. The tests were performed using the Gamry Instrument Potentiostat/Galvanostat/ZRA (REF 600) model. Working, counter, reference (mild steel coupon, a graphite bar) and a saturated calomel electrode (SCE), were the cell three electrodes. The DC105 and EIS300 software packages developed by (Gamry) were used to performed the EIS measurements, which start 30 min after immersed the coupon in the HCl solution to allow for the stabilization of the steady-state potential.

2.6 Surface characterization

Scanning electron microscopic (SEM) test was used to analysis the coupon surface without and with addition of the synthesized corrosion inhibitor. The mild steel coupon was firstly immersed in corrosive solution for 5 h at 303 K and secondly with addition of 0.5 mM of synthesized corrosion inhibitor. The mild steel samples were isolate, washed and dry to analysis the surface.

2.7 Quantum chemical calculations

The three-dimensional structure of DOBF as a reason which was responsible for the percentage of inhibition efficiency and significance of corroded technique upon the coupon surface. The study was carried out and compared with the methodological results [36-39]. Theoretical parameters such as *HOMO*, *LUMO*, energy gap (ΔE), atomic charges, dipole moment (μ), electron affinity (*A*), hardness (η), softness (σ) electronegativity (χ), ionization potential (*I*), and fraction of electrons transferred (ΔN) were determined by Density Functional Theory (DFT) calculations in addition to Mulliken atomic charge.

3. RESULTS AND DISCUSSION

The reaction sequence synthesis of the novel inhibitor namely 4-((5,5-dimethyl-3-oxocyclohexenyl)amino)benzenesulfonamide which derived from sulfanilamide and 5,5-dimethyl-cyclohexane-1,3-dione is summarized in Scheme 1. DOBF was synthesized by reflux of amounts of sulfanilamide with 5,5-dimethyl-cyclohexane-1,3-dione. The ¹H-NMR spectrum showed a singlet at δ 1.00 ppm due to the two groups of three CH₃ protons. Also, a doublet at 2.08 due to the tow NH₂ protons. A doublet at δ 2.22 ppm due to the two CH₂ protons and a doublet due to the tow CH₂ protons at δ 2.24 ppm. A singlet at δ 5.64 ppm single proton for vinyl group.

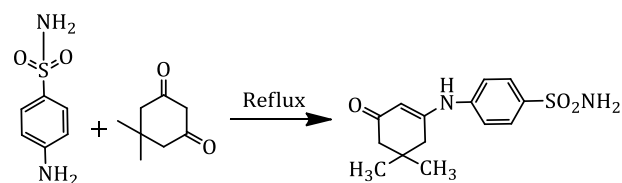


Fig. 1. Synthesis of the corrosion inhibitor DOBF.

3.1. Concentration effect

Weight loss of mild steel at different time period, in absence of various concentrations of DOBF in one molar of hydrochloric acid environment at 303K have been investigated. The values of inhibition efficiencies (IEs %) and corrosion rates (C_{RS}) are demonstrated in Figs. 2 and 3. It is obvious that the diminishing CR is correlated with increase in the DOBF concentration that elucidates that additional DOBF molecules are adsorbed on the surface of mild steel, thereby providing bigger surface coverage.

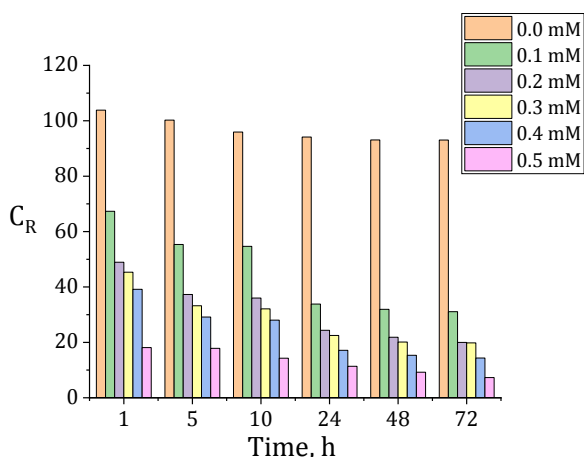


Fig. 2. Influence of DOBF concentration and time on corrosion rate of mild steel at 303 K.

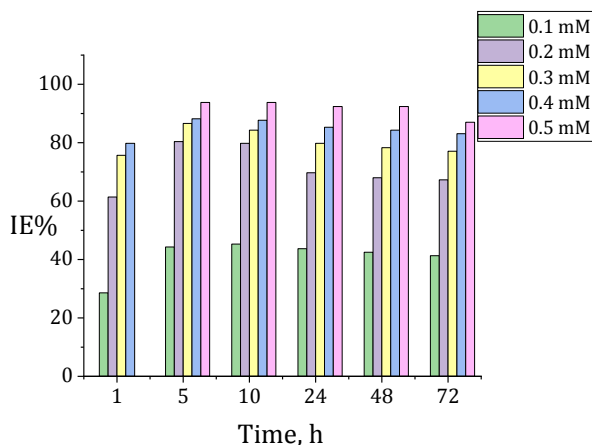


Fig. 3. Influence of DOBF concentration and time on IE% of mild steel at 303 K.

Figure 2 demonstrate the difference of CRs against exposure. The curves acquired suggest progressive decrease in CR with increase in inhibitor concentration. It could be spotted that for all studied concentrations of the DOBF utilized the corrosion rate of the mild steel decreased with time throughout the methodological interval.

3.2. Temperature effect

Temperature influence on inhibition reaction of corrosive environment mild steel surface is quite complicated, due to considerable effects might happen on the mild steel surface, like immediate etching, laceration, desorption of inhibitor and inhibitor molecules decomposition.

Temperature has a considerable impact on the corrosion rate of mild steel. Corrosion in an corrosive environment, the CR increases with increasing temperature due to the spread of hydrogen protons in the acidic environment over potential reductions. At all events assumed that in the acid corrosion the inhibitor molecules adsorb on the mild steel surface, producing in a structural variation of the double-layer and diminutive rate of the reaction. In industries some processes such as acid cleaning and pickling and the best temperature is of individual significance as temperature vary the interaction between the surface of mild steel and the corrosive environment without and with inhibitor. Inhibitor molecules that are of adsorptive kind the temperature difference affect the mild steel dissolution in addition to the degree of mild steel surface coverage by molecules of tested inhibitor at a steady value of their highest investigated concentration.

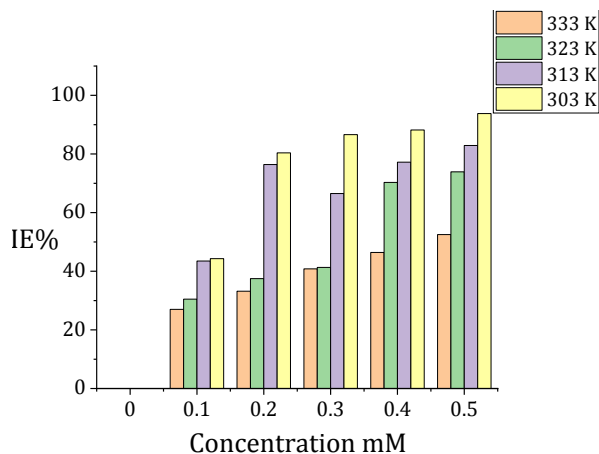


Fig. 4. Effect of temperature on inhibition efficiency of various DOBF concentrations.

To analysis the stability of the DOBF inhibitor molecules at higher temperature, measurements have been done at various temperature of 303, 313, 323 and 333K in one molar HCl environment. The obtained inhibition efficiencies result are in the Fig. 4. A significant decrease in metal corrosion was observed with the increasing

concentration of DOBF as tested corrosion inhibitor at tested temperatures.

The superior efficiency was found to be 93.8 % at 303K for 0.5 mM concentration of the DOBF inhibitor. This increase in inhibition efficiency with decrease in temperature propose the chemical adsorption of the DOBF inhibitor molecules on the corrosion surface.

Adsorption process of DOBF molecules, the adsorption heat is at all events negative, so this specified an exothermic reaction. This is why the inhibition efficiencies decreases at a highest tested temperature.

3.3. Electrochemical impedance spectroscopy measurements

Figure 5 shows the characteristics of the DOBF at the concentrations range 0.1 mM to 0.5 mM in corrosive environment at the examined temperature 303 K, as using EIS. On the other hand, Fig. 6 Shows equivalent circuit model, containing Rs (solution resistance), Rp (polarization resistance) and CPE (fixed phase element), as illustrates in equation (3):

$$Z_{CPE} = Y_o^{-1}(j\omega)^{-n} \quad (3)$$

where n match to the phase shift, which was connecting with the in-homogeneity of the double layer.

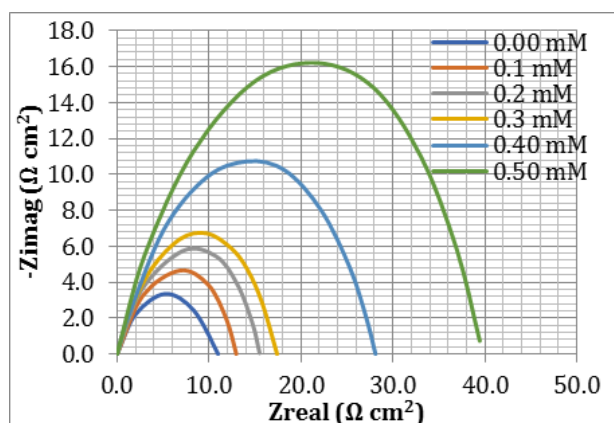


Fig. 5. The Nyquist plot for MS coupon in a 1 M HCl at 303 K, with various DOBF concentrations.

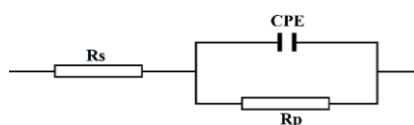


Fig. 6. Equivalent circuit used to fit the impedance spectra of a Nyquist plot for MS in a 1 M HCl.

For n = 0, CPE shows a resistance, for n = 1, a capacitance (C) and for n = -1 an inductance. The “double layer capacitance” values (C_{dl}) are calculated by eq. 4:

$$C_{dl} = Y_o(w_m'')^{n-1} \quad (4)$$

where ω'' is the angular frequency of impedance spectrum.

The impedance parameters are demonstrating in Table 1 and the inhibitive efficiencies (h) were measured via equation 5:

$$\eta(\%) = \frac{R_p - R_p^0}{R_p} \times 100 \quad (5)$$

where R_p and R_p⁰ are the DOBF (Ω cm²) with and without of various DOBF concentrations respectively.

Table 1. The EIS parameters for MS in HCl with and without of various DOBF concentrations.

Conc. (mM)	R _{ct} (ohm cm ²)	IE (%)
0.0	51.35	0.00
0.1	314.93	51.73
0.2	422.93	66.01
0.3	491.12	73.85
0.4	644.03	82.99
0.5	789.84	93.7

From Fig. 6, it is clear that the Nyquist Figure illustrates a depressed capacitive loop, but with addition of DOBF concentration, the capacitive loop radius will increase, that means that the charge transfer between the solution and coupon surface is dramatically hindered through the increase of the concentration of DOBF [40,41]. It is clear from Table 1 that the addition of DOBF as corrosion inhibitor, the R_p⁰ increases, which imply that the DOBF molecules have clear inhibition effects after adsorption on the coupon surface, when increase of DOBF concentration the electric double layer capacitance value were decreases, that is due to the DOBF molecules replacing the molecules of H₂O adsorbed on the coupon surface.

3.4. Morphology effect

The investigated surface morphology of mild steel in absent and presence DOBF molecules as corrosion inhibitor in 1 M HCl environment have been investigated by scanning electron microscopy technique. The SEM micrograph for the surface of MS of inhibitor in HCl is corroded and rough due to corrosion attack as demonstrates in Fig. 7a. On the other hand, the

inhibitor molecules presence with concentration of 0.5 mM demonstrates uniform passive protective film cover the mild steel surface due to the inhibitor molecules adsorbed on the mild steel surface from the environment as demonstrates in Fig. 7b. The scanning electron microscopy for the MS surface in presence of tested inhibitor award perfect protective film because of the potent and steady adsorption, that demonstrate the superior inhibitive action. This study suggests that the mild steel surface damages in corrosive environment. The presence of inhibitor molecules will protect the MS surface through the attack of corrosion because of the found protective barrier on mild steel surface.

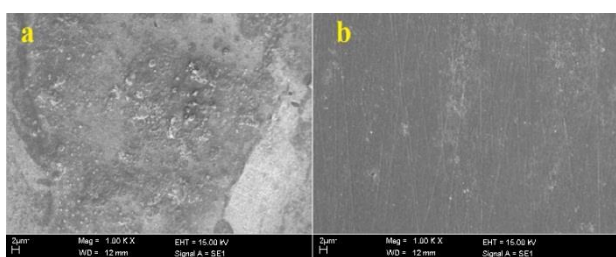


Fig. 7. The SEM micrographs for mild steel HCl with 0.5 mM of the corrosion inhibitor at 303 K for 5 h as immersion time. (a) absence the inhibitor; (b) in presence the inhibitor.

3.5. Adsorption isotherm effect

Adsorption isotherms: Usually it is aprovable that the naural and organic compounds have the ability to prevent the corrosion through adsorption at the surface alloy/solution interface and that the potential of adsorption depend on the structure of the studied inhibitor molecules, type of corrosive environment, nature of alloy surface, temperature of solution and electrochemical potential at the alloy/solution interface. The nature of inhibitor interact on the damage surface through corrosion inhibition of mild steel is concluded in terms of adsorption characteristics of studied inhibitor molecules. Surface coverage (θ) values are quite significant when searchng the adsorption properties and it is calculated by using equation 6.

$$\theta = IE\%/100 \quad (6)$$

3.6. Langmuir effect

Langmuir adsorption Isotherm have been investigated for its fit to the methodological work as in equation 7:

$$\theta = \frac{K_{eq} \times C_{conc.}}{1 + K_{eq}} \quad (7)$$

Equation 4 may be modified to equation 8:

$$\frac{C_{inh}}{\theta} = \frac{1}{K_{ads}} + C_{inh} \quad (8)$$

A plot of C / θ versus C was a straight line it follows Langmuir adsorption Isotherm. Figure 8, imply that DOBF as studied inhibitor was under Langmuir adsorption isotherm. The high K value reveals that the DOBF as studied inhibitor is strongly adsorbed on the surface of mild steel in corrosive environment.

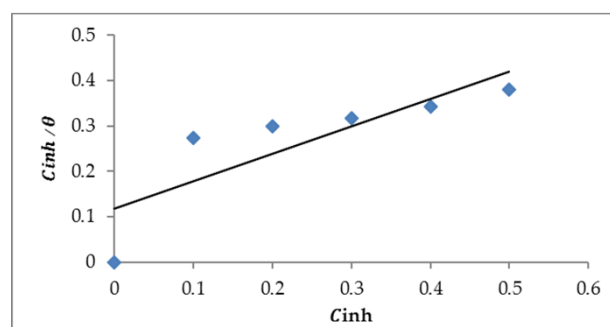


Fig. 8. Adsorption isotherm for mild steel in 1.0 M HCl with different concentrations of the DOBF as corrosion inhibitor.

3.7. Activation Process

The DOBF molecules were de-sorption of from the coupon surface at rising temperature (from 303 to 333 K), so the inhibition efficiency decreases. The relation of corrosion rate (CR), activation energy (E_a), temperature (T) and gas constant named Arrhenius equation (equation 9).

$$CR = A \exp\left(\frac{-E_a}{RT}\right) \quad (9)$$

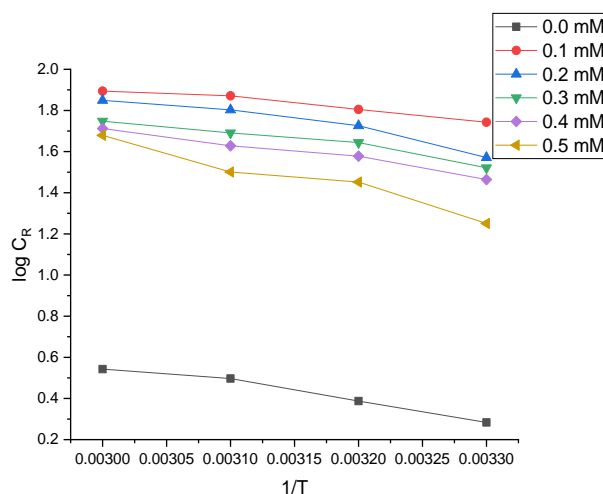


Fig. 9. Arrhenius plot for coupon corrosion without and with addition of various concentrations of DOBF.

The gravimetric analysis gave a straight line of the plot of log of CR vs 1/T as in Fig. 9 for investigated coupon in corrosive solution with various DOBF concentrations.

The $-E_a/2.303R$ represent the slope of plot for Figure 8 and the activation energy E_a value was listed in Table 2.

Table 2. Activation Parameters of investigated coupons in acidic solution in without and with addition of various concentrations of DOBF at different Temperature.

Conc. (mM)	E_a (kJ/mol)	ΔH_{corr}^* (kJ/mol)	$-\Delta S_{corr}^*$ (J/Mol.K)
0.0	16.74	13.95	188.84
0.1	24.11	19.02	174.14
0.2	25.30	21.27	170.43
0.3	26.52	23.85	161.92
0.4	29.82	28.51	158.51
0.5	31.89	30.92	145.94

The values activation energies of the studied coupons in acidic media in presence of DOBF are more than the value of activation energy in absence of the value. Table 2 displayed the rised of E_a with increase of DOBF concentration, and the C_R decrease. The enthalpy (ΔH_{corr}^*) and entropy (ΔS_{corr}^*) have been calculated according to equation 10.

$$CR = \frac{RT}{N_A h} \exp\left(\frac{\Delta S_{corr}^*}{R}\right) \exp\left(\frac{\Delta H_{corr}^*}{RT}\right) \quad 10$$

where Planck's constant the Avogadro number were represented by h and N_A respectively.

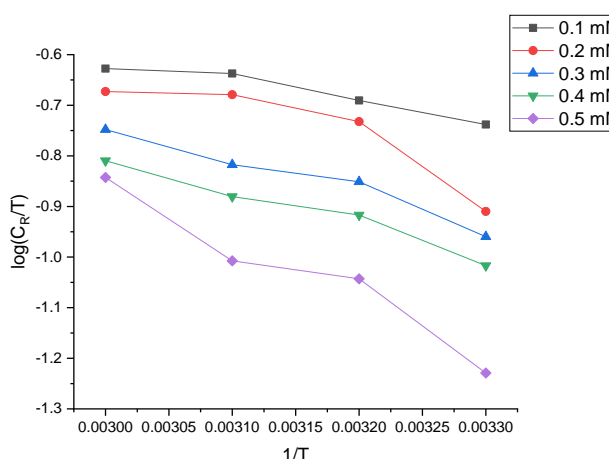


Fig. 10. Arrhenius plot for corrosion of tested coupon in acidic media with various conc. of DOBF.

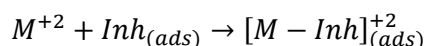
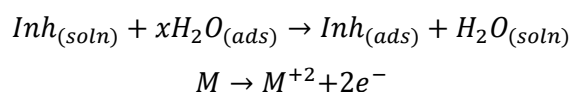
Figure 10 displayed the plot of $\log(CR/T)$ vs $1/T$ obtained for examined coupons in acidic media without and with addition of different

concentrations of DOBF gave straight line and the slope and intercept were $-\Delta H_{corr}^* / 2.303R$ and $[\log(R/NAh) + \Delta S_{corr}^* / 2.303R]$ respectively. ΔH_{corr}^* and ΔS_{corr}^* were obtained from Figure 8 and were displayed in Table 2.

The value of ΔS_{corr}^* have been increased with raising of DOBF concentration that suppose randomly reaction. The value of ΔH_{corr}^* that have positive value indicate the endothermic nature of the mild steel dissolution process proposing slow dissolution rate of surface coupon with increasing of DOBF concentration. Also, the values E_a and ΔH have increased with the increasing DOBF concentration suggest that the protective film increases.

3.8. Suggested Mechanism

The mechanism of adsorption of organic compounds as corrosion inhibitors at mild steel coupon/environment interface fellow steps. 1st step, inhibitor molecules adsorp on a coupon surface through replace with of H_2O molecules [42].



where $Inh(soln)$ and $Inh(ads)$ are the inhibitors that were adsorb on the coupon surface, x is water moles displaced with inhibitor molecules.

Inhibitor molecules can bond with M^{+2} on coupon surface as a result of iron dissolution or oxidation process, producing iron-inhibitor complex [43]:

The relative solubility of the metal-inhibitor complex can prevent or induce metal decay. It is generally accepted that without addition of corrosion inhibitors, the corrosive environment is always in contact with the coupon surface and porous film leading to corrosion as a result of the dissolution of the minerals, while in the presence of an inhibitor solution, active or open sites in the porous film are almost blocked by adsorption of the inhibitor leading to the presence of a barrier or a negative layer that suppresses additional corrosion. The phenomenon of adsorption is the major characteristics that demonstrate the

mechanism of inhibition. The adsorption influenced by the surface charge of the mild steel, interaction type between DOBF as inhibitor and mild steel surface in addition to the molecular structure of DOBF. The DOBF molecule has donor atoms (electronegative) nitrogen and oxygen in addition to pi-electrons of the benzene and pyrone rings. These donor sites cause efficient adsorption of inhibitor molecules onto the surface of tested coupons. In the mineral and halogenic acid environment, N atom become protonated because of hydration, chloride ions with a smaller degree adsorb at the electrode/environment interface, produce more negatively charge in the vicinity of the electrode/ environment interface, and prefer an excess adsorption of the positive charge protonated DOBF molecules (tested corrosion inhibitor) Inhibitor was adsorbed on the surface of mild steel and produce a film which has the ability to protect the surface of mild steel or the inhibitor molecules react chemically with the mild steel surface and form coordination bonds. The adsorption mechanism of natural and organic inhibitor molecules can perform through the following, electrostatical reaction between charged inhibitor molecules and mild steel surface and/or the interaction of π -electrons and/or electron pairs with the mild steel surface. Inhibitor molecules protect the mild steel surface by blocking anodic and/or cathodic reactions and forming insoluble metal complex. The inhibitive efficiencies of tested corrosion inhibitor versus the corrosion of surface of mild steel in corrosive environment can be demonstrated according to the adsorption sites number, size of molecule, charge density, type of interaction with the mild steel surface and potency to form of coordination complex. The electron pairs of sulfur, oxygen and nitrogen atoms in addition pi-bonds form chemical bonds with the mild steel surface as demonstrated in Fig. 11.

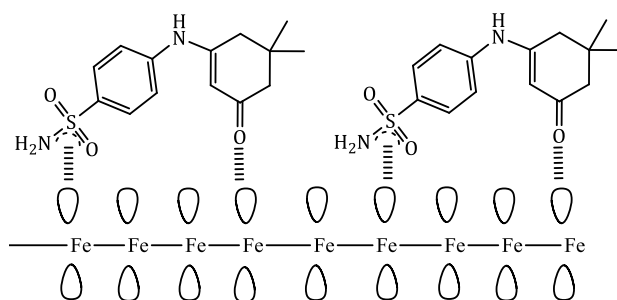
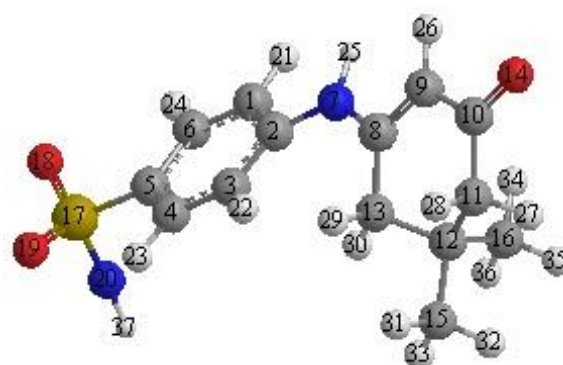


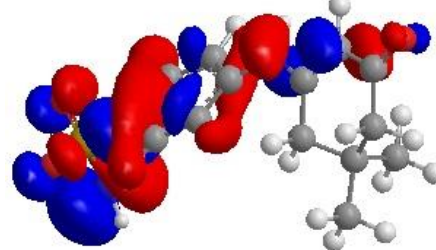
Fig. 11. The suggested mechanism of action of the DOBF as corrosion inhibitor.

3.9. Quantum chemical calculations of neutral inhibitor molecules

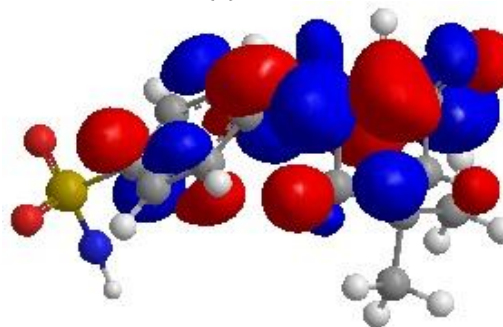
The quantum chemical parameters have been investigated by DFT method. The calculated parameters namely HOMO, LUMO (Fig. 12) and dipole moment (μ) have been studied and listed in Table 3. EHOMO is the electron donating ability of the molecules. Thus, the highest value of EHOMO refer to a major affinity for the donation of electrons to unoccupied molecular orbital that was d-orbital of iron atoms. Corrosion inhibition efficiency of the DOBF, E_{HOMO} , E_{LUMO} and dipole moment (μ) is shown in Table 3.



(a) Optimized structure



(b) HOMO



(c) LUMO

Fig. 12. Electronic properties of DOBF (a) optimization, (b) HOMO orbital, and (c) LUMO orbital.

As is observed that the inhibition efficiency increases with an increase in E_{HOMO} values along with a decrease in E_{LUMO} values. The increasing values of E_{HOMO} imply a superior tendency to

donate electrons to the molecule with empty orbitals. The dipole moment (μ) of the DOBF is -4.8047, suggest that DOBF molecules behave as strong inhibitor for the surface of mild steel. Density Functional Theory (DFT) has been found to be successful in providing insights into the chemical reactivity and selectivity in terms of global parameters such electron affinity (A), ionization potential (I), chemical softness (s), electronegativity (χ) and fraction of electrons transferred (ΔN) as quantum chemical parameters [16].

Table 3. Calculated quantum properties for the most stable conformation of DOBF.

Function	Values
EHOMO	-0.37 Hartree
ELUMO	-0.12 Hartree
EHOMO – ELUMO	-0.257 Hartree
f_{max}^-	0.152
f_{max}^+	0.098
Dipole Moment (μ)	-4.8 debye
$I = -EHOMO$ (hartree)	0.3770 Hartree
$A = -ELUMO$ (hartree)	0.1196 Hartree
$\eta = -0.5(E_{HOMO} - E_{LUMO})$	0.1332
$\sigma = 1/\eta$	7.5075
$\chi = -0.5(E_{HOMO} + E_{LUMO})$	0.2483
$\Delta N = -\frac{\Phi - \chi_{inh}}{2(\eta_{Fe} + \eta_{inh})}$	0.2953

Chemical hardness and softness are significant factors to measure the stability and reactivity of a molecule. It is obvious that the hardness generally indicates the resistance towards the deformation or polarization of the electron cloud of molecules under small perturbation of chemical reaction. A hard molecule has energy gaps with high values and a soft molecule have energy gaps with low values [34]. Inhibitor with low hardness value is expected to have the superior inhibition efficiency that is in comfortable with our study [35]. High electronegativity and low variation of electronegativity expected low reaction is which in turn indicates low inhibitory efficiency. The calculated fraction of electrons transferred, ΔN for DOBF. The values of ΔN demonstrate inhibition impact resulting from electrons donation that approbate with Lukovits et al. 'S study. If $\Delta N < 3.6$, the obligation efficiency increased with the increasing electron-donating ability at the metal surface.

3.10. Mullikan atomic charge

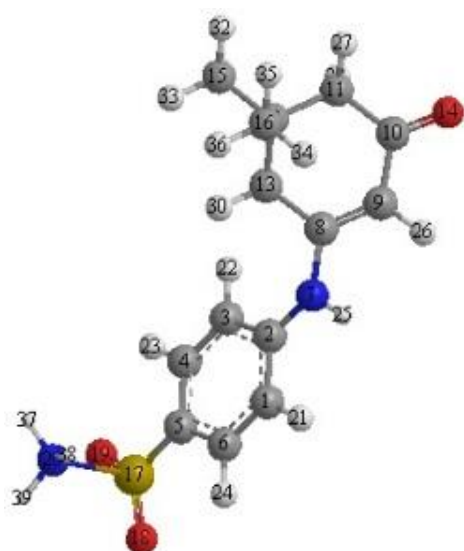
Earlier theoretical study on corrosion of Bentiss 2000, demonstrate that the presence of nitrogen, oxygen and sulfur as heteroatoms in the molecular structure of the inhibitor have the ability to bonded chemically with metal via coordination bonds and form coordination complex through the un shared of electron pairs of heteroatoms and un outbid d-orbital of the metal [36]. Similar case is displayed in DOBF. The negative charge on nitrogen atom (N20) is higher in DOBF than the other atoms and it is -0.954. The other two oxygen atoms (O18 and O19) were -0.9404 and -0.9414 respectively. A calculated theoretical data on Mullikan charges is demonstrate in Table 4.

Table 4. Mullikan charges of DOBF.

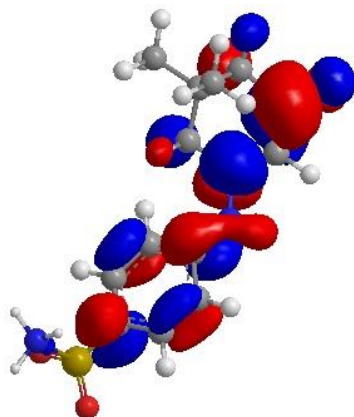
Atom	Charge	Atom	Charge
C(1)	-0.2193	C(11)	-0.2062
C(2)	0.1554	C(12)	-0.0429
C(3)	-0.2171	C(13)	-0.1378
C(4)	0.0170	O(14)	-0.3048
C(5)	-0.8754	C(15)	-0.2090
C(6)	0.0250	C(16)	-0.2106
N(7)	-0.2816	S(17)	2.8745
C(8)	0.1164	O(18)	-0.9404
C(9)	-0.3310	O(19)	-0.9414
C(10)	0.2767	N(20)	-0.9546

3.11. Quantum chemical calculations of protonated inhibitor molecules

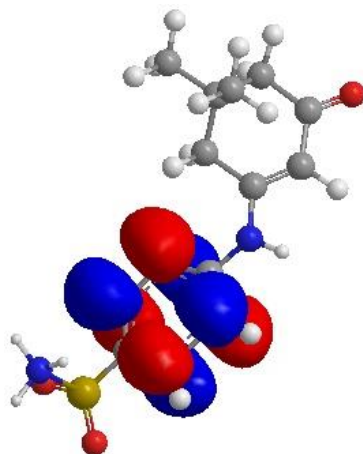
Heteroatoms such as nitrogen, oxygen and sulfur having more negative values of Mullikan charge is likely to undergo protonation easily. For the tested inhibitor DOBF it is not easy to loss proton. From the chemical structure of DOBF it is obvious that this compound is strong organic acid due to resonance, electron with drawing of SO₂ group and α,β -unsaturated carbonyl compound. Even herein we demonstrate the protonated form of the tested inhibitor DOBFH⁺. The optimized and electronic structures (HOMO and LUMO) are demonstrate in Fig. 13. Table 5 reveals that, the EHOMO and ELUMO value of DOBFH⁺ is less negativity compared to that of neutral DOBF. The EHOMO was shifted to less negative charge. It suggests that after protonation, the electron donating capability of DOBFH⁺ decreased.



(a) Optimized structure



(b) HOMO



(c) LUMO

Fig. 13. Electronic properties of protonated inhibitor molecules (a) optimization, (b) HOMO orbital, and (c) LUMO orbital.

All these factors cause the change in HOMO and LUMO distribution as compared to the neutral form. The obtained results as in Table 5, the ΔE (-0.1137 Hartree) was found for DOBFH⁺ as corrosion inhibitor and this is low amount.

Dipole moment (μ) of the DOBFH⁺ is significant parameter to determine the inhibition efficiency of the DOBFH⁺ for mild steel in acidic environment. The inhibition efficiency for mild steel by the inhibitor +molecules increase with the increasing dipole moment value. Corrosion inhibition efficiency of the DOBFH⁺, E_{HOMO} , E_{LUMO} and dipole moment (μ) is shown in Table 5. As is observed that the inhibition efficiency increases with an increase in E_{HOMO} values along with a decrease in E_{LUMO} values. The decreasing value of E_{HOMO} imply a DOBFH⁺ has low tendency to donate electrons to the molecule with empty orbitals. The dipole moment (μ) of the DOBFH⁺ is -1.05, suggest that DOBFH⁺ behave as inhibitor with low inhibition efficiency for the surface of mild steel. Density Functional Theory (DFT) has been found to be successful in providing insights into the chemical reactivity and selectivity in terms of global parameters such electron affinity (A), ionization potential (I), chemical softness (s) and electronegativity (χ) as quantum chemical parameters. These parameters were calculated for DOBFH⁺ and illustrate in Table 5.

Table 5. Calculated quantum properties for the most stable conformation of DOBFH⁺.

Function	Values
E_{HOMO}	-0.132Hartree
E_{LUMO}	-0.0183 Hartree
$E_{HOMO} - E_{LUMO}$	0.1137 Hartree
Dipole Moment (μ)	-1.05debye
$I = -E_{HOMO}$ (hartree)	0.132Hartree
$A = -E_{LUMO}$ (hartree)	0.05685Hartree
$\eta = -0.5(E_{HOMO} - E_{LUMO})$	-0.053
$\sigma = 1/\eta$	17.59
$\chi = -0.5(E_{HOMO} + E_{LUMO})$	-0.07515

3.12. Mullikan atomic charge of protonated inhibitor molecules (DOBFH⁺)

The negative charge on nitrogen atom (O19) higher in DOBFH⁺ than the other atoms and it is -0.8607. The other oxygen and Nitrogen atoms (O18 and N20) were -0.8598 and -0.4971 respectively. A calculated theoretical data on Mullikan charges is demonstrate in Table 6. It is obvious that the differences between DOBF and DOBFH⁺ is the negative charge of Nitrogen atom (N20). For DOBF it is higher than DOBFH⁺ about -0.457. This value confirm that the inhibition efficiency for DOBF is twice compare with DOBFH⁺.

Table 6. Mullikan charges of DOBFH⁺.

Atom	Charge	Atom	Charge
C(1)	-0.2376	C(11)	-0.2072
C(2)	0.2382	C(12)	-0.0402
C(3)	-0.2325	C(13)	-0.1350
C(4)	0.0604	C(14)	-0.2521
C(5)	-1.1119	O(15)	-0.2129
C(6)	0.0572	C(16)	-0.2144
N(7)	-0.2174	C(17)	2.8556
C(8)	0.0457	O(18)	-0.8598
C(9)	-0.2350	O(19)	-0.8607
C(10)	0.2630	N(20)	-0.4971

4. CONCLUSION

Results of the this study revealed that the new sulfanilamide namely 4-((5,5-dimethyl-3-oxocyclohexenyl) amino)benzenesulfonamide (DOBF) worked as an excellent corrosion inhibitor for surface of mild steel in hydrochloric acid solution in a concentration-dependent technique. IE of DOBF as corrosion inhibitor with superior inhibition efficiency of 93.8% at the concentration of 0.5 mM, and decreases with a increasing temperature, that proposed of physisorption. Inhibitor molecules were adsorbed on surface MS obeying the Langmuir isotherm. DOBF molecules are proved as superior inhibitor with good inhibitive characteristics due to presence of nitrogen, sulphur and oxygen atoms. SEM measurements confirming the forming of a protective layer by inhibitor molecules on the coupon surface. The anti-corrosion study of DOBF molecules, obviously implied its role in the protection of coupon surface in corrosive environment.

Acknowledgement

This study was supported by the University of Technology, Baghdad, Iraq.

REFERENCES

[1] M. Benarioua, A. Mihi, N. Bouzeghaia, M. Naoun, *Mild steel corrosion inhibition by Parsley (Petroselinum Sativum) extractin acidic*, Egyptian Journal of Petroleum, vol. 28, iss. 2, pp. 155–159, 2019, doi: 10.12739/NWSA.2019.14.3.3A0090

[2] K.F. Khaled, *The inhibition of benzimidazole derivatives on corrosion of iron in 1 M HCl solutions*, Electrochimica Acta, vol. 48, iss. 17, pp. 2493–2503, 2003, doi: 10.1016/S0013-4686(03)00291-3

[3] R.M. Castro, L.C.C. Cavaler, F.M. Marques, V.M. Bristot, A.S. Rocha, *Comparative of the Tribological Performance of Hydraulic Cylinders Coated by the Process of Thermal Spray HVOF and Hard Chrome Plating*, Tribology in Industry, vol. 36, no. 1, pp. 79-89, 2014.

[4] V.S. Sastri, *Green corrosion inhibitors: theory and practice*. John Wiley & Sons Ltd, 2011.

[5] G. Skordaris, K.D. Bouzakis, T. Kotsanis, P. Charalampous, *A Critical Review of Measures for an Effective Application of Nano-Structured Coatings in Milling*, Tribology in Industry, vol. 39, no. 2, pp. 211-218, 2017, doi: 10.24874/ti.2017.39.02.08

[6] A. Fiala, A. Chibani, A. Darchen, A. Boulkamh, K. Djebbar, *Investigations of the inhibition of copper corrosion in nitric acid solutions by ketene dithioacetal derivatives*, Applied Surface Science, vol. 253, iss. 24, pp. 9347–9356, 2007, doi: 10.1016/j.apsusc.2007.05.066

[7] R. Javaherdashti, *How Corrosion Affects Industry and Life*, Anti-Corrosion Methods and Materials, vol. 47, no. 1, pp. 30–34, 2000, doi: 10.1108/00035590010310003

[8] S. Junaedi, A. Kadhum, A. Al-Amiery, A. Mohamad, M. Takriff, *Synthesis and characterization of novel corrosion inhibitor derived from oleic acid: 2-Amino-5-Oleyl-1,3,4-Thiadiazol (AOT)*, Interantional Journal of Electrochemical Science, vol. 7, pp. 3543–3554, 2012.

[9] A.S Fouda, A.M. Eldesoky, M.A. Diab, A. Nabih, *Inhibitive, Adsorption Studies on Carbon Steel Corrosion in Acidic Solutions by New Synthesized Benzene Sulfonamide Derivatives*, International Journal of Electrochemical Science, vol. 11, pp. 9998 – 10019, 2016.

[10] A. A. Al-Amiery, A. A. H. Kadhum, A. B. Mohamad, S. Junaedi, *A Novel Hydrazinecarbothioamide as a Potential Corrosion Inhibitor for Mild Steel in HCl*, Materials, vol. 6, iss. 4, pp. 1420–1431, 2013, doi: 10.3390/ma6041420

[11] A. Al-Amiery, A. Kadhum, A. Mohamad, A. Musa, C. Li, *Electrochemical study on newly synthesized chlorocurcumin as an inhibitor for mild steel corrosion in hydrochloric acid*, Materials, vol. 6, iss. 12, pp. 5466–5477, 2013, doi: 10.3390/ma6125466

[12] H. Cang, Z. Fei, W. Shi, Q. Xu, *Experimental and theoretical study for corrosion inhibition of mild*

- steel by L-Cysteine, *Interantional Journal of Electrochemical Science*, vol. 7, pp. 10121–10131, 2012.
- [13] A.A.H. Kadhum, A.B. Mohamad, L.A. Hammed, A.A. Al-Amiery, N.H. San, A.Y. Musa, *Inhibition of Mild Steel Corrosion in Hydrochloric Acid Solution by New Coumarin*, *Materials*, vol. 7, iss. 6, pp. 4335–4348, 2014, doi: [10.3390/ma7064335](https://doi.org/10.3390/ma7064335)
- [14] A.A. Al-Amiery, A.A.H. Kadhum, A. Kadhim, A.B. Mohamad, C.K. How, S. Junaedi, *Inhibition of Mild Steel Corrosion in Sulfuric Acid Solution by New Schiff Base*, *Materials*, vol. 7, iss. 2, pp. 787–804, 2014, doi: [10.3390/ma7020787](https://doi.org/10.3390/ma7020787)
- [15] A.A. Al-Amiery, A.A.H. Kadhum, A.H.M. Alobaidy, A.B. Mohamad, P.S. Hoon, *Novel Corrosion Inhibitor for Mild Steel in HCl*, *Materials*, vol. 7, iss. 2, pp. 662–672, 2014, doi: [10.3390/ma7020662](https://doi.org/10.3390/ma7020662)
- [16] A. Mohamad, A. Kadhum, A. Al-Amiery, L. Ying, A. Musa, *Synergistic of a coumarin derivative with potassium iodide on the corrosion inhibition of aluminum alloy in 1.0M H₂SO₄*, *Metals and Materials Interanational*, vol. 20, iss. 20, pp. 459–467, 2014, doi: [10.1007/s12540-014-3](https://doi.org/10.1007/s12540-014-3)
- [17] H.R. Obayes, G.H. Alwan, A.H.M.J. Alobaidy, A.A. Al-Amiery, A.A.H. Kadhum, A.B. Mohamed, *Quantum chemical assessment of benzimidazole derivatives as corrosion Inhibitors*, *Chemistry Central Journal*, vol. 8, no. 21, pp. 1–8, 2014, doi: [10.1186/1752-153X-8-21](https://doi.org/10.1186/1752-153X-8-21)
- [18] A.A. Al-Amiery, Y.K. Al-Majedy, A.A.H. Kadhum, A.B. Mohamad, *New Coumarin Derivative as an Eco-Friendly Inhibitor of Corrosion of Mild Steel in Acid Medium*, *Molecules*, vol. 20, iss. 1, pp. 366–383, 2015, doi: [10.3390/molecules20010366](https://doi.org/10.3390/molecules20010366)
- [19] E. Yousif, Y. Win, A. Al-Hamadani, A. Al-Amiery, A. Kadhum, A. Mohamad, *Furosemi as an environmental-friendly inhibitor of corrosion of zinc metal in acid medium experimental and theoretical studies*, *Interantional Journal of Electrochemical Science*, vol. 10, iss. 2, pp. 1708–1718, 2015.
- [20] A. Rubaye, A. Abdulwahid, S. Al-Baghdadi, A. Al-Amiery, A. Kadhum, A. Mohamad, *Cheery sticks plant extract as a green corrosion inhibitor complemented with LC-EIS/ MS spectroscopy*, *Interantional Journal of Electrochemical Science*, vol. 10, iss. 10, pp. 8200–8209, 2015.
- [21] A. Al-Obaidy, A. Kadhum, S. Al-Baghdadi, A. Al-Amiery, A. Kadhum, E. Yousif, *Eco-friendly corrosion inhibitor: experimental studies on the corrosion inhibition performance of creatinine for mild steel in HCl complemented with quantum chemical calculations*, *Interantional Journal of Electrochemical Science*, vol. 10, iss. 5, pp. 3961–12972, 2015.
- [22] S.B. Al-Baghdadi, F.T.M. Noori, W.K. Ahmed, A.A. Al-Amiery, *Thiadiazole as a Potential Corrosion Inhibitor for Mild Steel in 1 M HCl*, *Journal of Advanced Electrochemistry*, vol. 2, iss. 1, pp. 67–69, 2016.
- [23] A.A. Al-Amiery, F.A.B. Kassim, A.A.H. Kadhum, A.B. Mohamad, *Synthesis and characterization of a novel eco-friendly corrosion inhibition for mild steel in 1 M hydrochloric acid*, *Science Reports*, vol. 6, pp. 1–13, 2016, doi: [10.1038/srep19890](https://doi.org/10.1038/srep19890)
- [24] A. Kadhim, A.K. Al-Okbi, D.M. Jamil, A. Qussay, A.A. Al-Amiery, T.S. Gaaz, A.A.H. Kadhum, A.B. Mohamed, M.H. Nassir, *Experimental and theoretical studies of benzoxazines corrosion inhibitors*, *Results in Physics*, vol. 7, pp. 4013–4019, 2017, doi: [10.1016/j.rinp.2017.10.027](https://doi.org/10.1016/j.rinp.2017.10.027)
- [25] R. Obayes, A. Al-Amiery, G. Alwan, T. Abdullah, A. Kadhum, A. Mohamad, *Sulphonamides as corrosion inhibitor: experimental and DFT studies*, *Journal of Molecular Structure*, vol. 1138, pp. 27–34, 2017, doi: [10.1016/j.molstruc.2017.02.100](https://doi.org/10.1016/j.molstruc.2017.02.100)
- [26] S.B. Al-Baghdadi, F.G. Hashim, A.Q. Salam, T.K. Abed, T.S. Gaaz, A.A. Al-Amiery, A.A.H. Kadhum, K.S. Reda, W.K. Ahmed, *Synthesis and corrosion inhibition application of NATN on mild steel surface in acidic media complemented with DFT studies*, *Results in Physics*, vol. 8, pp. 1178–1184, 2018, doi: [10.1016/j.rinp.2018.02.007](https://doi.org/10.1016/j.rinp.2018.02.007)
- [27] H. Habeeb, H. Luaibi, R. Dakhil, A. Kadhum, A. Al-Amiery, T. Gaaz, *Development of new corrosion inhibitor tested on mild steel supported by electrochemical study*, *Results Phys*, vol. 8, pp. 1260–1267, 2018, doi: [10.1016/j.rinp.2018.02.015](https://doi.org/10.1016/j.rinp.2018.02.015)
- [28] K.F. Al-Azawi, I.M. Mohammed, S.B. Al-Baghdadi, T.A. Salman, H.A. Issa, A.A. Al-Amiery, T.S. Gaaz, A.A.H. Kadhum, *Experimental and quantum chemical simulations on the corrosion inhibition of mild steel by 3-((5-(3,5- dinitrophenyl)-1,3,4-thiadiazol-2-yl)imino)indolin-2-one*, *Results in Physics*, vol. 9, pp. 278–283, 2018, doi: [10.1016/j.rinp.2018.02.055](https://doi.org/10.1016/j.rinp.2018.02.055)
- [29] D.M. Jamil, A.K. Al-Okbi, S.B. Al-Baghdadi, A.A. Al-Amiery, A. Kadhim, T.S. Gaaz, *Experimental and theoretical studies of Schiff bases as corrosion inhibitors*, *Chemistry Central Journal*, vol. 12, no. 7, pp. 1–7, 2018, doi: [10.1186/s13065-018-0376-7](https://doi.org/10.1186/s13065-018-0376-7)
- [30] M. Ahmed, A. Al-Amiery, Y. Al-Majedy, A. Kadhum, A. Mohamad, T. Gaaz, *Synthesis and characterization of a novel organic corrosion inhibitor for mild steel in 1 M hydrochloric acid*, *Results in Physics*, vol. 8, pp. 728–733, 2018, doi: [10.1016/j.rinp.2017.12.039](https://doi.org/10.1016/j.rinp.2017.12.039)
- [31] T.A. Salman, D.S. Zinad, S.H. Jaber, M. Al-Ghezi, A. Mahal, M.S. Takriff, A.A. Al-Amiery, *Effect of 1,3,4*

Thiadiazole Scaffold on the Corrosion Inhibition of Mild Steel in Acidic Medium: An Experimental and Computational Study, Journal of Bio- and Tribo-Corrosion, vol. 5, iss. 48, pp. 1–11, 2019, doi: [10.1007/s40735-019-0243-7](https://doi.org/10.1007/s40735-019-0243-7)

- [32] D.M. Jamil, A.K. Al-Okbi, M.M. Hanon, K.S. Rida, A.F. Alkaim, A.A. Al-Amiery, A. Kadhim, A.A.H. Kadhum, *Carbethoxythiazole corrosion inhibitor: As an experimentally model and DFT theory*, Journal of Engineering and Applied Sciences, vol. 13, iss. 11, pp. 3952-3959, 2018, doi: [10.36478/jeasci.2018.3952.3959](https://doi.org/10.36478/jeasci.2018.3952.3959)
- [33] ASTM G77-98, *Standard Test Method for Ranking Resistance of Materials to Sliding Wear Using Block-on-Ring Wear Test*, 1998.
- [34] A.Y. Issa, K.S. Rida, A.Q. Salam, A.A. Al-Amiery, *Acetamidocoumarin as a based eco-friendly corrosion inhibitor*, International Journal of ChemTech Research, vol. 9, no. 11, pp. 39-47, 2016.
- [35] H.J. Habeeb, H.M. Luaibi, T.A. Abdulah, R.M. Dakhil, A.A.H. Kadhum, A.A. Al-Amiery, *Case study on thermal impact of novel corrosion inhibitor on mild steel*, Case studies in thermal engineering, vol. 12, pp. 64-68, 2018, doi: [10.1016/j.csite.2018.03.005](https://doi.org/10.1016/j.csite.2018.03.005)
- [36] W. Zhang, H. Li, M. Wang, L. Wang, A. Zhang and Y. Wu, *Highly effective inhibition of mild steel corrosion in HCl solution by using pyrido[1,2-a]benzimidazoles*, New Journal of Chemistry, vol. 43, iss. 1, pp. 413-426, 2019, doi: [10.1039/C8NJ04028A](https://doi.org/10.1039/C8NJ04028A)
- [37] W. Zhang, H. Li, C. Wang, L. Wang, G. Li, H. Ma, Q. Pana, Y. Wu, *Synergistic effect of 1-(2,5-dioximidazolidin-4-yl)urea and Tween-80 towards the corrosion mitigation of mild steel in HCl*, New Journal of Chemistry, vol. 43, iss. 35, pp. 13899-13910, 2019, doi: [10.1039/C9NJ03336J](https://doi.org/10.1039/C9NJ03336J)
- [38] G. Dehghani, B. Bahlakeh, M. Ramezanzadeh, M. Ramezanzadeh, *A combined experimental and theoretical study of green corrosion inhibition of mild steel in HCl solution by aqueous Citrullus lanatus fruit (CLF) extract*, Journal of Molecular Liquids, vol. 279, pp. 603-624, 2019, doi: [10.1016/j.molliq.2019.02.010](https://doi.org/10.1016/j.molliq.2019.02.010)
- [39] B. Tan, S. Zhang, H. Liu, Y. Guo, Y. Qiang, W. Li, L. Xu, S. Chen, *Corrosion inhibition of X65 steel in sulfuric acid by two food flavorants 2-isobutylthiazole and 1-(1,3-Thiazol-2-yl) ethanone as the green environmental corrosion inhibitors: Combination of experimental and theoretical researches*, Journal of Colloid and Interface Science, vol. 538, pp. 519-529, 2019, doi: [10.1016/j.jcis.2018.12.020](https://doi.org/10.1016/j.jcis.2018.12.020)
- [40] F. Bentiss, M. Traisnel, M. Lagrenee, *The Substituted 1,3,4-oxadiazoles: a New Class of Corrosion Inhibitors of Mild Steel in Acidic Media*, Corrosion Science, vol. 42, iss. 1, pp. 127–146, 2000, doi: [10.1016/S0010-938X\(99\)00049-9](https://doi.org/10.1016/S0010-938X(99)00049-9)
- [41] J.O'M. Bockris, D.A.J. Swinkels, *Adsorption of n-Decylamine on Solid Metal Electrodes*, Journal of the Electrochemical Society, vol. 111, iss. 6, pp. 736–743, 1964, doi: [10.1149/1.2426222](https://doi.org/10.1149/1.2426222)
- [42] E.E. Oguzie, Y. Li, F.H. Wang, *Corrosion inhibition and adsorption behavior of methionine on mild steel in sulfuric acid and synergistic effect of iodide ion*, Journal of Colloid and Interface Science, vol. 310, iss. 1, pp. 90-98, 2007, doi: [10.1016/j.jcis.2007.01.038](https://doi.org/10.1016/j.jcis.2007.01.038)
- [43] A.Y. Et-Etre, *Natural honey as corrosion inhibitor for metals and alloys. i. copper in neutral aqueous solution*, Corrosion Science, vol. 40, iss. 11, pp. 1845–1850, 1998, doi: [10.1016/S0010-938X\(98\)00082-1](https://doi.org/10.1016/S0010-938X(98)00082-1)